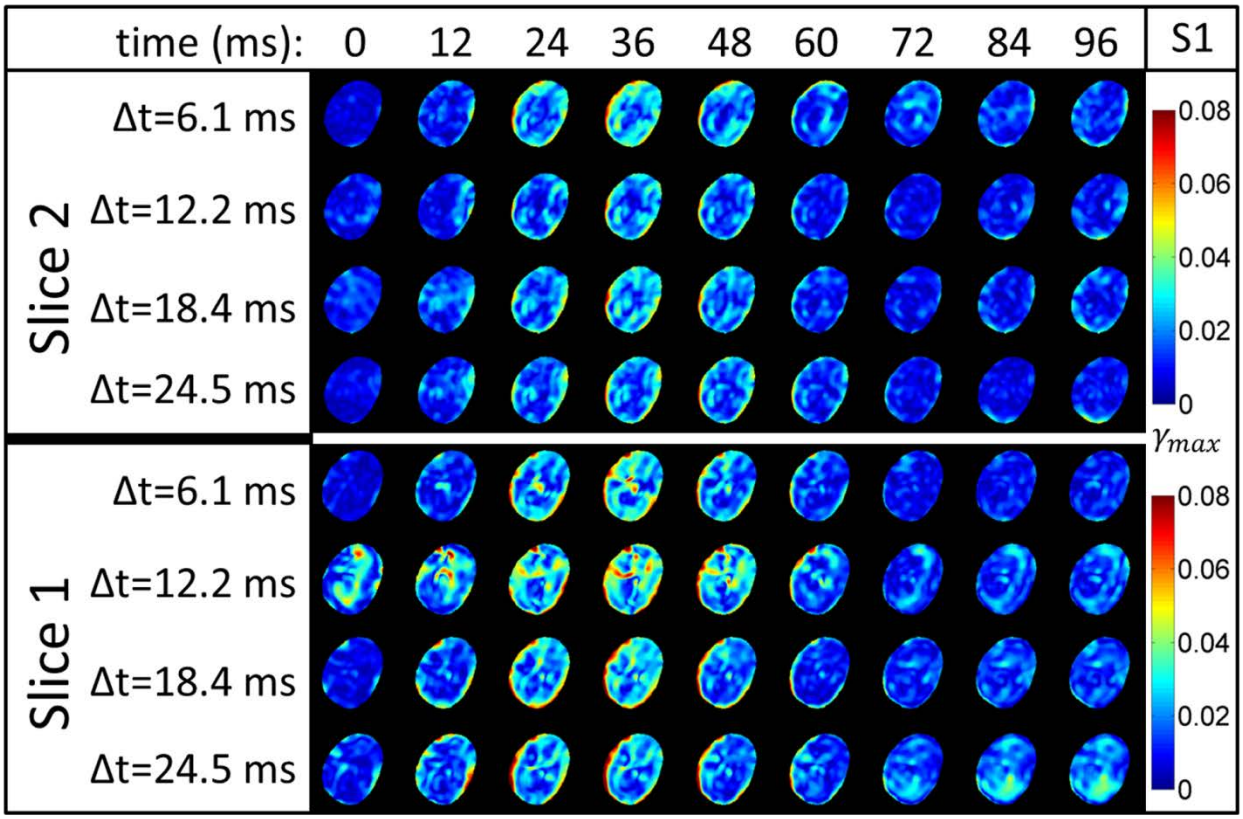

Supplemental Figure 1: The effect of temporal sampling resolution on estimates of maximum shear strain, γ_{max}, in subject 1 for the first 96 ms after impact. The number of rotations required decreases in inverse proportion to temporal sampling resolution from N=24 (Δt = 6.1 ms) to N=6 (Δt = 24.5 ms).

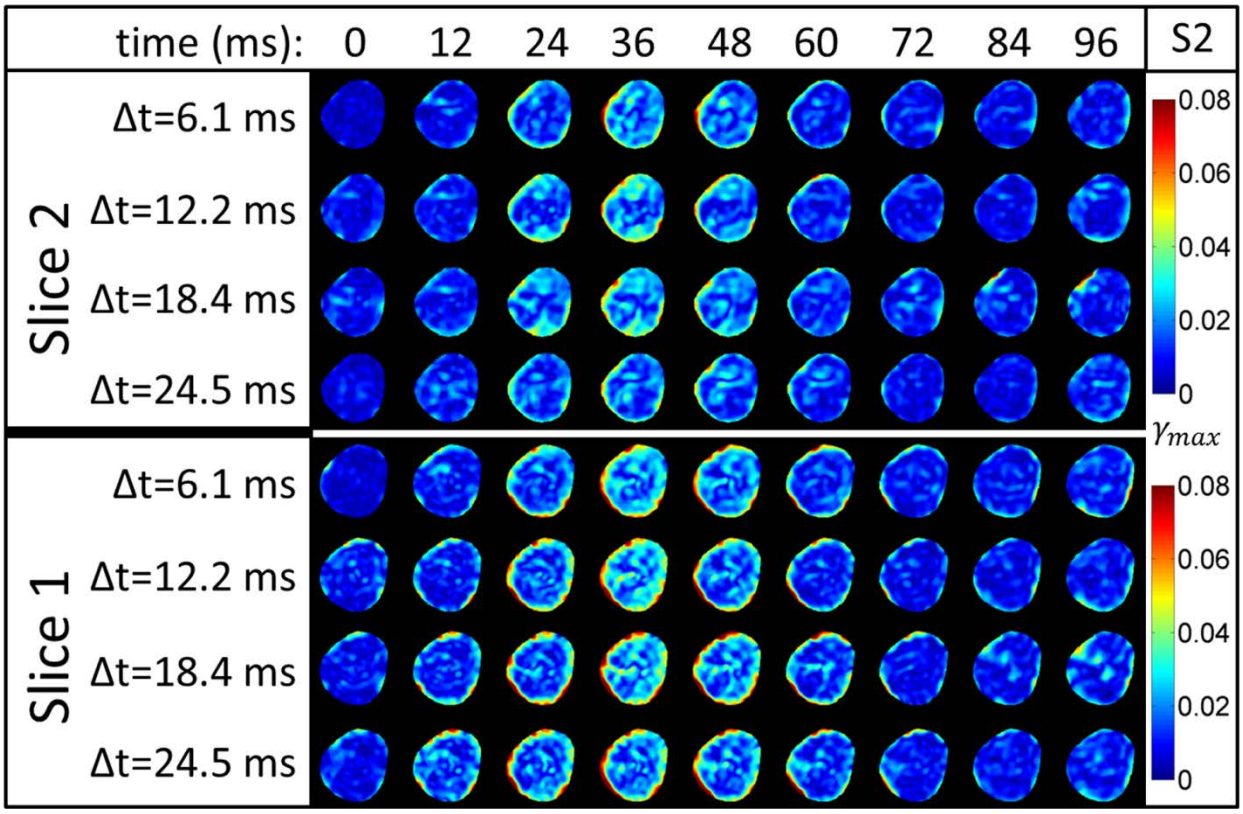

Supplemental Figure 2: The effect of temporal sampling resolution on estimates of maximum shear strain, γ_{max}, in subject 2 for the first 96 ms after impact. The number of rotations required decreases in inverse proportion to temporal sampling resolution from N=24 (Δt = 6.1 ms) to N=6 (Δt = 24.5 ms).

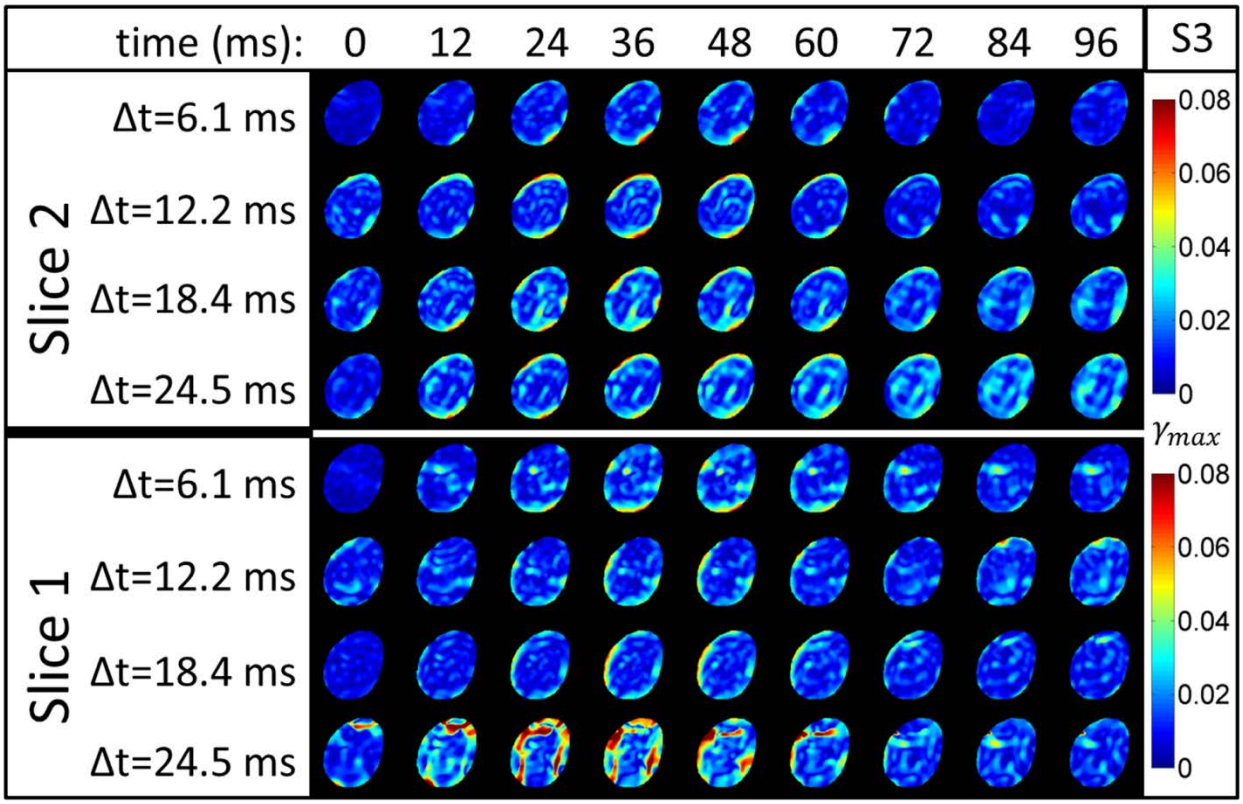

Supplemental Figure 3: The effect of temporal sampling resolution on estimates of maximum shear strain, γ_{max}, in subject 3for the first 96 ms after impact. The number of rotations required decreases in inverse proportion to temporal sampling resolution from N=24 (Δt = 6.1 ms) to N=6 (Δt = 24.5 ms).

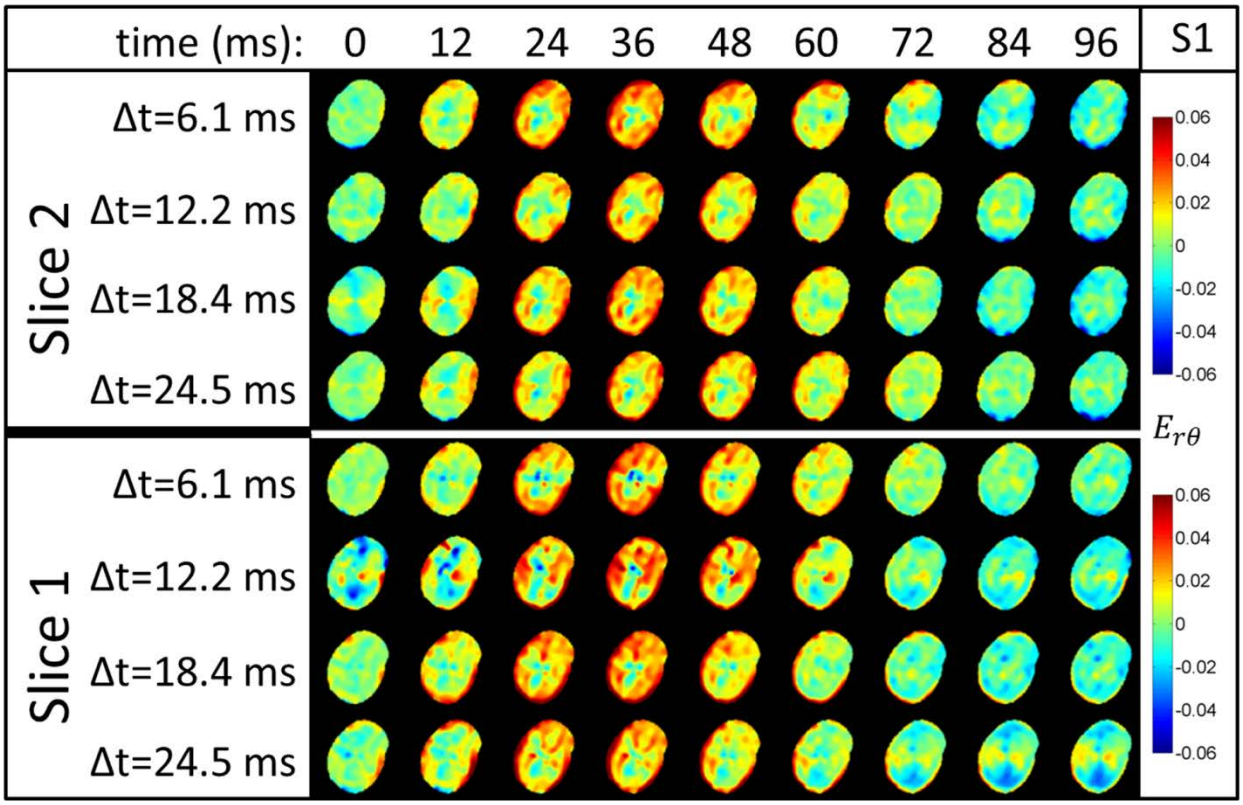

Supplemental Figure 4: The effect of temporal sampling resolution on estimates of radial-circumferential shear strain, $E_{r\theta}$, in subject 1 for the first 96 ms after impact. The center of rotation was identified manually by plotting the computed displacements between the first two image frames. Displacements were measured with respect to the reference configuration, so the same center of rotation was used for all acquired time frames.

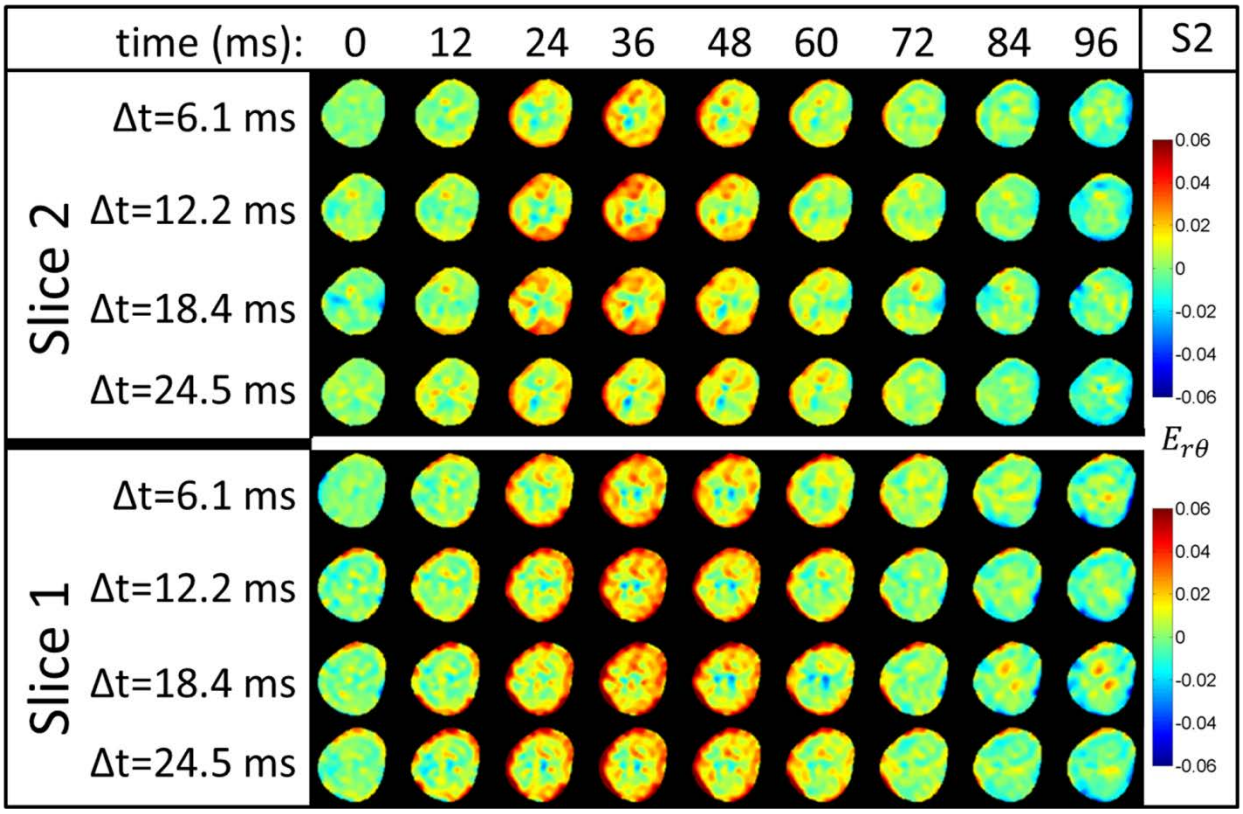

Supplemental Figure 5: The effect of temporal sampling resolution on estimates of radial-circumferential shear strain, $E_{r\theta}$, in subject 2 for the first 96 ms after impact.

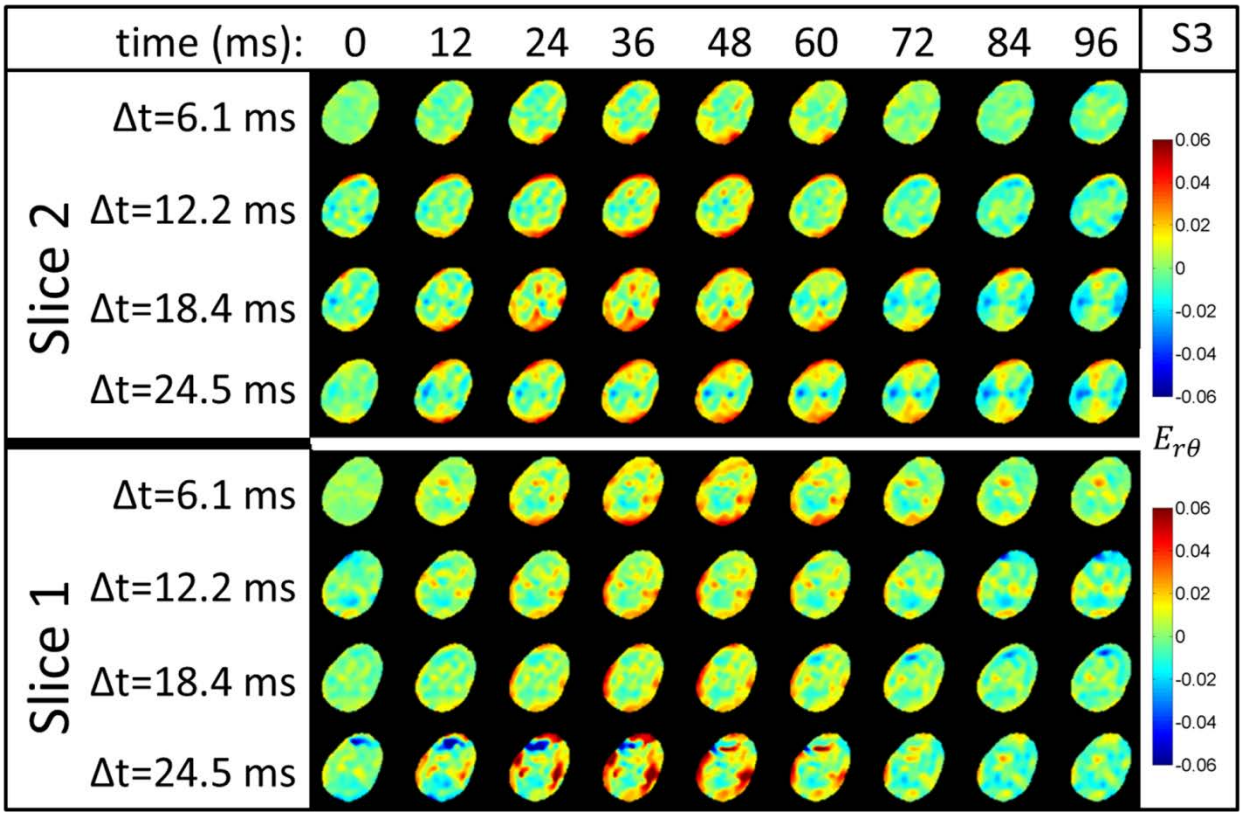

Supplemental Figure 6: The effect of temporal sampling resolution on estimates of radial-circumferential shear strain, $E_{r\theta}$, in subject 3 for the first 96 ms after impact.